Absolute determination of optical constants by reflection electron energy loss spectroscopy

H. Xu,[1] B. Da,[2] J. Tóth,[3] K. Tőkési,[3,4,*] and Z. J. Ding[1,†]

[1]*Key Laboratory of Strongly-Coupled Quantum Matter Physics, Chinese Academy of Sciences and Hefei National Laboratory for Physical Sciences at Microscale and Department of Physics, University of Science and Technology of China, Hefei 230026, Anhui, People's Republic of China*

[2]*Center for Materials Research by Information Integration, National Institute for Materials Science, Tsukuba, Ibaraki 305-0047, Japan*

[3]*Institute for Nuclear Research, Hungarian Academy of Sciences (ATOMKI), P.O. Box 51, Debrecen, Hungary*

[4]*ELI-ALPS, ELI-HU Non-profit Ltd., Dugonics tér 13, H-6720 Szeged, Hungary*

(Received 20 September 2016; published 16 May 2017)

We present an absolute extraction method of optical constants of metal from the measured reflection electron energy loss spectroscopy spectra with the help of a recently developed reverse Monte Carlo technique. The method is based on a direct physical modeling of electron transportation with an optimization procedure of the energy loss function (ELF). The optical constants and the electron inelastic mean free path were obtained after verifying the accuracy of the derived ELF with the *f*- and *ps*-sum rules. This approach provides a valid and universal tool to investigate intrinsic properties of metals by using the electron energy loss spectroscopy technique.

DOI: 10.1103/PhysRevB.95.195417

I. INTRODUCTION

There is a continuous interest and effort in the determination of optical constants of solids due to their importance in both fundamental research and applications. For this purpose, optical methods based on reflectance and absorption spectroscopy as well as spectroscopy ellipsometry are the most extensively employed approaches, by which the measured data for metals and semiconductors are compiled to form a popular database of optical constants [1,2]. However, many materials still lack the data in the intermediate photon energy range around 20–50 eV. Furthermore, the available data in the current database usually consist of various energy regions measured by different groups and means; thereby the data may not be smoothly joined. On the other hand, the electron energy loss spectroscopy [3–5] can provide an alternative way for deriving information about the dielectric response of a solid to an external electric field carried by electrons, which is, in principal, a rather different technique compared with optical methods. In recent years a well established technique based on the reflection electron energy loss spectroscopy (REELS) has been developed [6–16] to obtain optical constants in a rather wide range of energy loss of electrons (i.e., photon energy). The typical energy loss range is 1–100 eV, and the measurements can be performed once or maybe several times under different experimental conditions but with the same spectrometer. Such an ability to derive optical constants in a wide photon energy range with only one spectrum is the main advantage of REELS compared with the optical measurements. In addition, it also holds the opportunity to get the optical constants for nonzero momentum transfers.

In deriving the energy loss function (ELF), $\mathrm{Im}[-1/\varepsilon(\omega)]$, and thereby the optical constants (n,k), where $\varepsilon = n + ik$ is the complex dielectric function of the solid, from the measured REELS spectra, precise and accurate knowledge of the electron energy loss processes has crucial importance. Electron interaction with a sample is comprised of the electron elastic scattering and the bulk- as well as surface-electronic excitation for electron inelastic scattering. Among the various strategies for the extraction of optical constants from a REELS spectrum, many of the previous works [6–8,16] used an analytical algorithm [17] to get the single inelastic scattering distribution, i.e., the differential inverse inelastic mean free path (DIIMFP), by neglecting the influence of the elastic scattering completely. Since the ELF is directly related to the DIIMFP, such a treatment was later modified to compensate for the influence of elastic scatterings by applying a scaling factor [9,10]. However, the obtained effective ELF has ambiguous physical meaning. In the same spirit, a REELS spectrum was analytically constructed as a convolution of multiple inelastic scattering distributions contributed by surface and bulk excitations [11,12,18]. The weighting factors for the corresponding energy loss distributions represent only the partial intensity of electrons inelastically scattered in the solid. Although these attempts have promoted advances in understanding of electron interactions with solid surfaces and have provided valuable optical data for some metals [12], this kind of analytical modeling still has serious problems: (a) Calculations require preknowledge as input of electron inelastic mean free path (IMFP) and surface excitation parameter (SEP), which actually are results determined by the optical constants (specifically by the ELF) of the sample; (b) although the REELS spectrum intensity is scaled with the elastic peak intensity, however, without taking account of the elastic scattering process exactly in the analysis of the measured spectrum the obtained ELF data are not absolute and, therefore, the ELF must be scaled by introducing artificial scaling factors [12]; (c) furthermore, the shape of the REELS spectrum is actually also sensitive to the ratio of cross sections between elastic and inelastic scattering, and thus electron elastic scattering also influences the derived ELFs; (d) lastly the analytical algorithm [12] which includes surface excitation assumes homogeneous scattering properties of a sample while the surface excitation is, in fact, depth dependent [19–21].

In our previous work [15] a reverse Monte Carlo (RMC) method, which integrates the Monte Carlo (MC) simulation

*tokesi@atomki.mta.hu
†zjding@ustc.edu.cn

of the REELS spectrum and the Markov chain Monte Carlo (MCMC) technique for updating of the ELF, was established to include elastic and multiple scattering effects in the evaluation of ELF from an experimental spectrum. The RMC method overcomes the drawbacks of various analytic methods in that (a) elastic scattering of electrons is taken into account completely, which consequently ensures the absolute determination of the ELF values rather than a relative one; (b) the multiple scattering effects including the surface excitation are taken into account in a well-developed MC technique [21], which has been proven to be the most accurate method so far for REELS spectrum analysis [22]. The absolute values of the optical constants were obtained successfully by the RMC method for SiO_2 in our previous work [15]; however, the use of a constant fitting parameter S for accounting of surface excitation effects approximately has inevitably limited potential application for solids with complex electronic structures, such as transition metals. The critical issue in our previous calculation was that S represents the depth independent surface excitation probability; this rough assumption makes the DIIMFP calculations relatively poor and limits the accuracy of the final quantitative evaluation of optical constants which are merely bulk property.

In the present work, the framework of the RMC method is extended to allow the MC modeling of the depth-dependent surface excitations in the simulation for a more sophisticated description of the electron inelastic scattering process. The surface mode of collective excitations [23] rises from the presence of a sample boundary between material and vacuum; the surface excitation probability should depend on the distance of electron position to the surface. A measured REELS spectrum is a superposition of energy losses due to bulk and surface modes and therefore must be decomposed. According to the previous investigations on the surface excitation effects [24–26], for accurate MC simulation of REELS spectrum one has to use directly a spatial- (depth- and directional-) dependent DIIMFP. Two typical models are available to calculate the DIIMFP, i.e., the semiclassical one [20,27] and the quantum mechanical one [28,29]. In this work, the semiclassical model is used, partly because it gives very close results with the quantum mechanical model in most cases [30], while more importantly it is computationally more efficient. REELS spectra of iron were measured for primary energies of 1000, 2000, and 3000 eV. The self-consistency of the ELFs was achieved with our RMC method. The accuracy of the ELF and the validity of the method were verified by comparing the obtained data with the literature and also by evaluating the f- and ps-sum rules. In addition to optical constants, the IMFP, which is more commonly measured by the elastic peak electron spectroscopy (EPES), was deduced as well based on the obtained ELF. This RMC method will certainly extend the quantitative ability of the REELS spectroscopy.

II. THEORY

A. Monte Carlo simulation

The main feature of the MC modeling of electron-solid interactions for a REELS spectrum consists of the use of Mott's cross section for electron elastic scattering and a dielectric response theory for electron inelastic scattering. Details of the sampling procedure of the electron flight length from a depth-dependent DIIMFP inside a sample and in vacuum, which is the key to the present simulation of multiple electron scattering, can be found in our previous work [21].

1. Elastic scattering

The relativistic expression of electron-atom scattering, i.e., Mott's cross section [31], is employed for the treatment of electron elastic scattering,

$$\frac{d\sigma}{d\Omega} = |f(\vartheta)|^2 + |g(\vartheta)|^2, \tag{1}$$

where the scattering amplitudes,

$$\begin{aligned} f(\vartheta) &= \frac{1}{2iK}\sum_{\ell=0}^{\infty}\{(\ell+1)(e^{2i\delta_\ell^+}-1) \\ &\quad + l(e^{2i\delta_\ell^-}-1)\}P_\ell(\cos\vartheta); \\ g(\vartheta) &= \frac{1}{2iK}\sum_{\ell=1}^{\infty}\{-e^{2i\delta_\ell^+}+e^{2i\delta_\ell^-}\}P_\ell^1(\cos\vartheta), \end{aligned} \tag{2}$$

are calculated by the partial wave expansion method [32]. $P_\ell(\cos\vartheta)$ and $P_\ell^1(\cos\vartheta)$ are the Legendre and the first-order associated Legendre functions. δ_ℓ^+ and δ_ℓ^- represent spin-up and spin-down phase shifts of the ℓth partial wave. In the calculation of the phase shifts, the Thomas-Fermi-Dirac atomic potential [33] is used and the atomic number of the sample is the only required input parameter.

2. Inelastic scattering

a. Bulk model. Under a homogeneous sample assumption and in the case of a fast electron moving inside an infinite sample, the electron inelastic scattering can be completely described by the dielectric theory via the bulk ELF, $\mathrm{Im}[-1/\varepsilon(\omega,q)]$. The differential inelastic cross section, i.e., DIIMFP, is given by

$$\frac{d^2\lambda_{\mathrm{in}}^{-1}}{d(\hbar\omega)dq} = \frac{1}{\pi a_0 E}\mathrm{Im}\left[\frac{-1}{\varepsilon(\omega,q)}\right]\frac{1}{q}, \tag{3}$$

where a_0 is the Bohr radius, $\hbar\omega$ and $\hbar q$ are, respectively, the energy loss and the momentum transfer for an electron of kinetic energy E. λ_{in} is the IMFP. In this scheme, only the bulk excitation mode is considered.

b. Surface model. Owing to the presence of a surface boundary at the interface of a bulk material and vacuum, surface excitation mode occurs. For the configuration of REELS measurement signal electrons penetrate the sample surface twice. A measured REELS spectrum is contributed by signal electrons which have gone through both bulk and surface excitations. In order to give a more accurate quantitative description of REELS spectrum, two typical models, namely, the semiclassical one [20,27] and the quantum mechanical one [28,29], were worked out to yield the depth-dependent DIIMFPs. In this work, the semiclassical model is employed for its higher numerical efficiency [30]. The expression of the depth-dependent DIIMFP containing both the bulk ELF term, $\mathrm{Im}[-1/\varepsilon(\omega,q)]$, and the surface ELF term,

$\mathrm{Im}[-1/(\varepsilon(\omega,q)+1)]$, is written as

$$\sigma(z) = \frac{2}{\pi v^2}\int_{q_-}^{q_+} dq\,\frac{1}{q}\mathrm{Im}\left[\frac{1}{\varepsilon(\vec{q},\omega)}\right]\Theta(-z) + \frac{4\cos\alpha}{\pi^3}\int_{q_-}^{q_+} dq\int_0^{\frac{\pi}{2}} d\theta\int_0^{2\pi} d\phi\,\frac{q\sin^2\theta\cos(q_\perp z)\exp(q_\parallel z)}{\tilde{\omega}^2+{q_\parallel}^2{v_\perp}^2}$$
$$\times\left\{\mathrm{Im}\left[\frac{-1}{\varepsilon(\vec{q}_\parallel,\omega)+1}\right]-\frac{1}{2}\mathrm{Im}\left[\frac{-1}{\varepsilon(\vec{q}_\parallel,\omega)}\right]\right\}\Theta(-z) + \frac{4\cos\alpha}{\pi^3}\int_{q_-}^{q_+} dq\int_0^{\frac{\pi}{2}} d\theta\int_0^{2\pi} d\phi\,\frac{q\sin^2\theta\exp(-q_\parallel z)}{\tilde{\omega}^2+{q_\parallel}^2{v_\perp}^2}$$
$$\times\mathrm{Im}\left[\frac{-1}{\varepsilon(\vec{q}_\parallel,\omega)+1}\right]\left[2\cos\left(\frac{\tilde{\omega}z}{v\cos\alpha}\right)-\exp(-q_\parallel z)\right]\Theta(z), \qquad v_\perp > 0 \tag{4}$$

and

$$\sigma(z) = \frac{2}{\pi v^2}\int_{q_-}^{q_+} dq\,\frac{1}{q}\mathrm{Im}\left[\frac{1}{\varepsilon(\vec{q},\omega)}\right]\Theta(-z) + \frac{4\cos\alpha}{\pi^3}\int_{q_-}^{q_+} dq\int_0^{\frac{\pi}{2}} d\theta\int_0^{2\pi} d\phi\,\frac{q\sin^2\theta\cos(-q_\perp z)\exp(-q_\parallel z)}{\tilde{\omega}^2+{q_\parallel}^2{v_\perp}^2}$$
$$\times\mathrm{Im}\left[\frac{-1}{\varepsilon(\vec{q}_\parallel,\omega)+1}\right]\Theta(z) + \frac{4\cos\alpha}{\pi^3}\int_{q_-}^{q_+} dq\int_0^{\frac{\pi}{2}} d\theta\int_0^{2\pi} d\phi$$
$$\times\frac{q\sin^2\theta\exp(q_\parallel z)}{\tilde{\omega}^2+{q_\parallel}^2{v_\perp}^2}\left\{\mathrm{Im}\left[\frac{-1}{\varepsilon(\vec{q}_\parallel,\omega)+1}\right]-\frac{1}{2}\mathrm{Im}\left[\frac{-1}{\varepsilon(\vec{q}_\parallel,\omega)}\right]\right\}\left[2\cos\left(\frac{\tilde{\omega}z}{v\cos\alpha}\right)-\exp(-q_\parallel z)\right]\Theta(-z), \qquad v_\perp < 0 \tag{5}$$

where $\tilde{\omega} = \omega - qv\sin\theta\cos\phi\sin\alpha$, $q_\parallel = q\sin\theta$, $v_\perp = v\cos\alpha$, for an electron penetrating the surface from the solid (or vacuum) side into the vacuum (or solid) side, respectively. The integral limits of q are determined by the energy and momentum conservation relations as $q_\pm = \sqrt{2E} \pm \sqrt{2(E-\omega)}$. Details of the derivation of the above DIIMFP can be found in our previous work [30].

B. Determination of optical constants

Since the inelastic scattering cross section of the signal electrons in a REELS spectrum is determined by the ELF, the dielectric function $\varepsilon(\omega,q)$, the relevant optical constants, and IMFP can therefore be evaluated from the measured REELS spectrum by the RMC method. In the RMC procedure, a trial ELF is parametrized as a sum of a number of Drude-Lindhard functions:

$$\mathrm{Im}\left[\frac{-1}{\varepsilon(q,\omega)}\right] = \sum_{i=1}^{N} A_i\,\mathrm{Im}\left[\frac{-1}{\varepsilon(q,\omega;\omega_{pi},\gamma_i)}\right], \tag{6}$$

where the $3N$ oscillator parameters, A_i, ω_{pi}, and γ_i, are, respectively, the oscillator strength, the energy, and the width of the ith oscillator. They are arbitrarily selected for the long wavelength limit, $q \to 0$, as the initial input. For finite q values, the dielectric function $\varepsilon(q,\omega)$ is extended from the long wavelength limit, namely, the optical dielectric function $\varepsilon(\omega)$, via Ritchie and Howie's scheme [34]. Based on the first set of the oscillator parameters, a MC simulation is performed to produce an initial simulated REELS spectrum, $I_0^{\mathrm{sim}}(\Delta E)$. A "goodness" of the oscillator parameters after n iterations is defined as

$$\chi_n^2 = \sum_j \left[I_n^{\mathrm{sim}}(\Delta E_j) - I^{\mathrm{exp}}(\Delta E_j)\right]^2\sigma(\Delta E_j)^2, \tag{7}$$

where $I^{\mathrm{exp}}(\Delta E_j)$ is the experimental intensity and $\sigma(\Delta E_j)$ is a weighting factor to specify the importance at an interested energy loss ΔE_j. The optimal values of $3N$ oscillator parameters are determined by a successive procedure; i.e., the simulation of REELS spectrum is performed iteratively in order to minimize the goodness parameter, χ_n^2. In this way, the final ELF will converge and represent the true value of the sample. For materials having a complex shape of ELF, such as transition metals, about 50 or more Drude-Lindhard terms are necessary for an adequate expression of ELF. The determination of the ELF thus actually turns into a task of global optimization in a hyperspace of over 100 dimensions. The simulated annealing method (SA) [35], as one of the most popular probabilistic searching techniques for MCMC sampling, is employed for adjusting the parameter set to reduce computation time. In analogy to the annealing process to find the ground state of a crystalline condensed matter, χ_n^2 is regarded as the potential energy in SA. During the MCMC sampling process, a Boltzmann probability distribution $P(\Delta E) = \exp(-\Delta E/k_B T_n)$ is used as the acceptance function, where $\Delta E = \chi^2_{\mathrm{new}} - \chi^2_{\mathrm{old}}$ is the difference in the potential energy between the old step and a new trial step. In our calculation, the "temperature" is set with a fast annealing algorithm as $T_n(\Delta E_j) = T_0/(1+n)$, where T_0 is the initial value. In this way, the final optimized ELF, as a sum of Drude-Lindhard terms, is independent of the choice of the initial parameter set, as a basic property of the MCMC method.

Once the final ELF, $\mathrm{Im}[-1/\varepsilon(\omega)]$, is obtained by the RMC method, the real part, $\mathrm{Re}[-1/\varepsilon(\omega)]$, is deduced through an analytical Kramers-Kronig relation. Then the real and imaginary parts of the dielectric function can be obtained as, respectively,

$$\varepsilon_1 = \frac{-\mathrm{Re}[-1/\varepsilon(\omega)]}{\mathrm{Im}[-1/\varepsilon(\omega)]^2 + \mathrm{Re}[-1/\varepsilon(\omega)]^2},$$
$$\varepsilon_2 = \frac{\mathrm{Im}[-1/\varepsilon(\omega)]}{\mathrm{Im}[-1/\varepsilon(\omega)]^2 + \mathrm{Re}[-1/\varepsilon(\omega)]^2}. \tag{8}$$

Upon the complex dielectric function, the optical constants, n and k, can therefore be derived as

$$n = \sqrt{\frac{\varepsilon_1 + \sqrt{{\varepsilon_1}^2+{\varepsilon_2}^2}}{2}}, \quad k = \sqrt{\frac{-\varepsilon_1 + \sqrt{{\varepsilon_1}^2+{\varepsilon_2}^2}}{2}}. \tag{9}$$

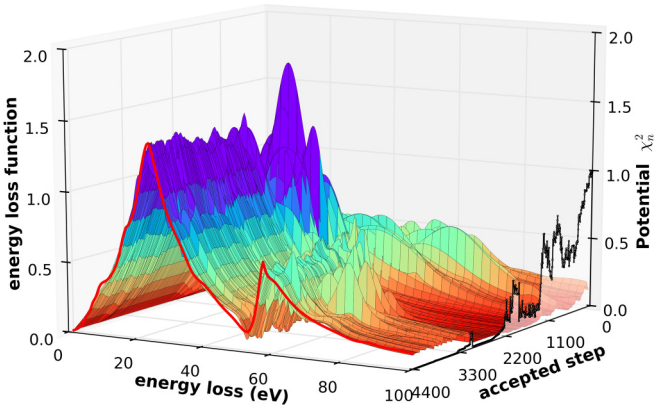

FIG. 1. Evolution of ELF in the RMC process, showing updating of the trail ELFs of Fe with MCMC iteration steps. The final ELF is depicted in red line. Variation of the "potential" is displayed by the black line.

III. EXPERIMENT

Three REELS spectra for a mechanically polished polycrystalline iron sheet sample were recorded with primary electron energies at 1000, 2000, and 3000 eV in an energy loss range of 0–100 eV by the home-built electron spectrometer ESA-31 at ATOMKI [36]. The analyzer works in a fixed retardation ratio mode with a relative energy resolution of 5×10^{-3}. In the present experiments the used pass energies were around 100 eV, and in this way the analyzer energy resolution was around 0.5 eV. The full widths at half maximum, being the convolution of the analyzer and the electron source generated widening of the elastic peak, were around 0.6–0.7 eV. The incident angle of the primary electron beam is 50° with respect to the surface normal of the sample and the angle of the analyzed electrons is 0° relative to the surface normal.

IV. RESULTS AND DISCUSSION

MC simulations for the REELS spectra were performed for this geometry and for the three primary electron energies. Figure 1 shows the evolution of the trial ELF as a function of the number of MCMC steps. The corresponding goodness parameter, χ_n^2, or equivalently the potential in the parameter, space changes with trial ELF at each step. The potential χ_n^2 curve shows a feature of local fluctuations while in an overall decline tendency. This is ensured by the MCMC samplings of the SA algorithm, whereas by applying the acceptance function of $P(\Delta E) = \exp(-\Delta E/k_B T)$ an equilibrium state of Boltzmann distribution shall be reached after the "melting" stage [23]. Moreover, as the "temperature" T cools down with iterative steps, the Boltzmann distribution eventually turns into the lowest energy state. For an intuitionistic view, the evolution of the optical constants is shown in Fig. 2, where the refractive index n and the extinction coefficient k are depicted each as a function of the RMC iteration steps, corresponding to the updating of ELFs in Fig. 1.

By the RMC algorithm each REELS spectrum measured under a certain experimental condition will yield an ELF of the sample. In this paper, we have performed calculations for three experimental spectra measured at 1000, 2000, and 3000 eV in order to check the consistency of the obtained ELFs. Figure 3(a) shows that the agreement between the final simulated and experimental REELS spectra on the absolute intensity scale is excellent, covering the whole range from the elastic peak down to an energy loss of 100 eV, for all three primary energies. Here the absolute intensity means that the spectrum is scaled with the intensity of the elastic peak, as shown in the inset of Fig. 3(a). To reveal the importance of surface excitations, we have calculated REELS spectra taking into account only the pure bulk excitation by employing the bulk model in Sec. II. Thus the contribution of surface excitations is derived by subtraction of the pure bulk contribution from the full spectra, as displayed in Fig. 3(a). One can see that at a lower primary energy the contribution from surface excitation becomes more important; this is because the surface excitation probabilty increases with lowering electron energy. Figure 3(b) shows the corresponding bulk ELF, $\mathrm{Im}[-1/\varepsilon(\omega)]$, and the related surface ELF, $\mathrm{Im}[-1/(\varepsilon(\omega)+1)]$, for the three energies determined in an absolute way by the RMC method, without resorting to any artificial normalization procedure. An overall consistency among the three ELFs has been gained as expected. To check the accuracy of these ELFs, f- and ps-sum

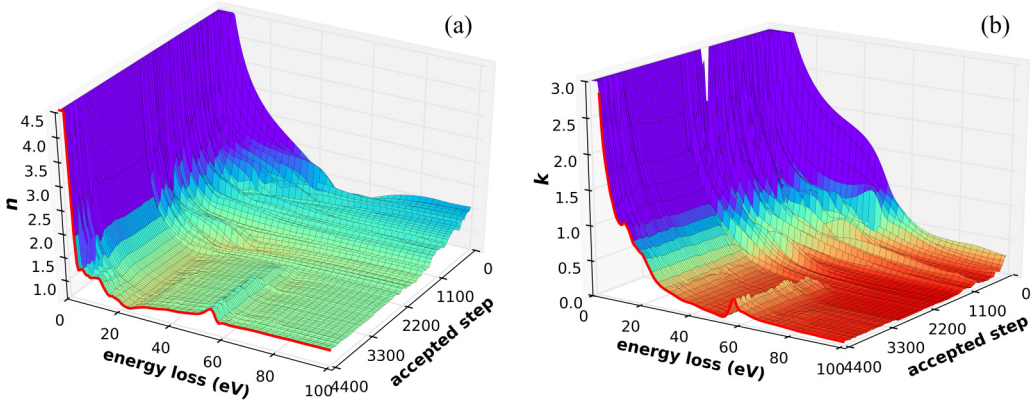

FIG. 2. Evolution of (a) the refractive index n and (b) the extinction coefficient k of Fe, corresponding to ELFs in Fig. 1, in the RMC process. The final values are shown with red lines.

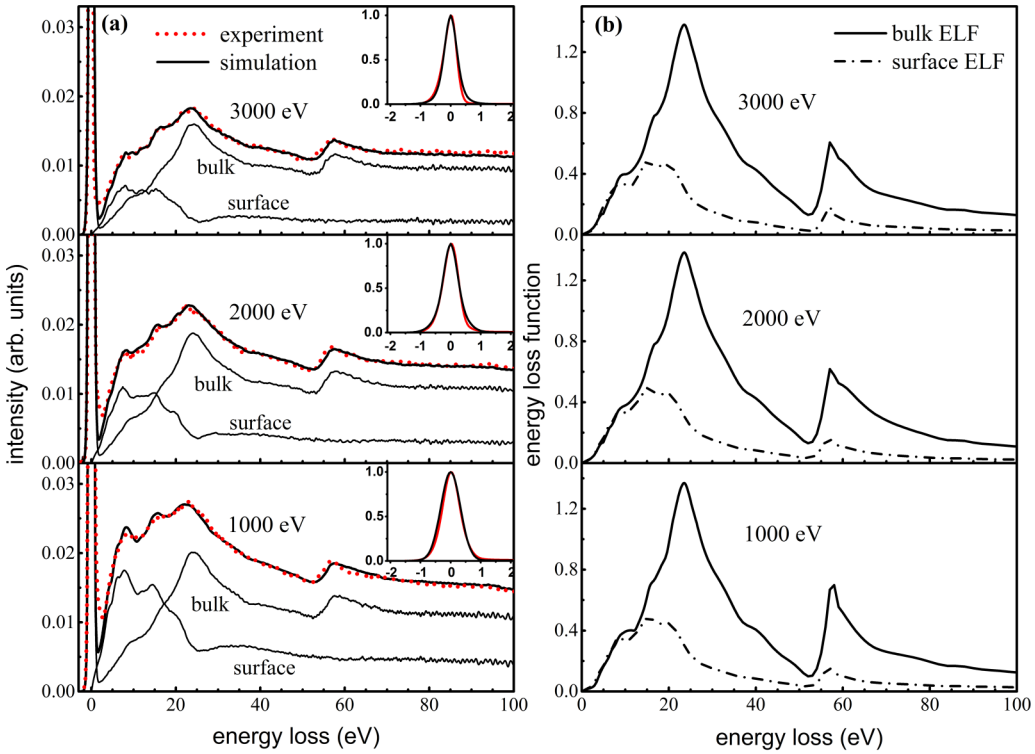

FIG. 3. (a) Comparison of simulated REELS spectra (solid lines) and measured spectra (dotted lined) of Fe at 1000, 2000, and 3000 eV. The inset shows the normalization on the elastic peak intensity. Contributions from bulk and surface excitations from MC simulation are illustrated as well. (b) The final bulk energy loss function, $\mathrm{Im}[-1/\varepsilon(\omega)]$, and the surface energy loss function, $\mathrm{Im}[-1/(\varepsilon(\omega)+1)]$, obtained from the REELS spectra for the corresponding energies by the RMC method.

rules were calculated, which are defined, respectively by,

$$Z_{\mathrm{eff}} = \frac{2}{\pi \Omega_p^2} \int_0^\infty \omega \mathrm{Im}[-1/\varepsilon(\omega)] d\omega, \tag{10}$$

$$P_{\mathrm{eff}} = \frac{2}{\pi} \int_0^\infty \frac{1}{\omega} \mathrm{Im}[-1/\varepsilon(\omega)] d\omega, \tag{11}$$

where $\hbar\Omega_p = \sqrt{4\pi n_a e^2/m_e}$ and n_a is the atomic density of the sample. The obtained results are summarized in Table I, where the data above 100 eV are taken from measurements performed by Henke *et al.* [37]. The nominal theoretical values for f- and ps-sum rules are the atomic number ($Z = 26$ for Fe) and 1, respectively. We found that for all three energies the obtained values are very close to the theoretical values; the relative errors are very small for both sum rules. This clearly indicates that our calculated ELFs give reasonable optical properties of the Fe sample from the near-visible to the soft x-ray photon energy region. Therefore, this agreement also confirms that the present MC modeling of electron interaction with solid surface is quite reasonable. The sum rules calculated taking an average over the three energies are also given in Table I.

TABLE I. List of f-sum and ps-sum rule checks for ELFs derived from REELS spectra at 1000, 2000, and 3000 eV and for averaged ELF (RMC).

Primary energy	Z_{eff} (f sum)	Relative error	P_{eff} (ps sum)	Relative error
1000 eV	25.95	−0.19%	1.024	2.4%
2000 eV	25.80	−0.76%	1.045	4.5%
3000 eV	26.24	0.92%	1.051	5.1%
RMC	25.99	−0.04%	1.040	4.0%

To minimize the uncertainties, we take an average over the ELFs for the three energies. Figure 4 shows the averaged

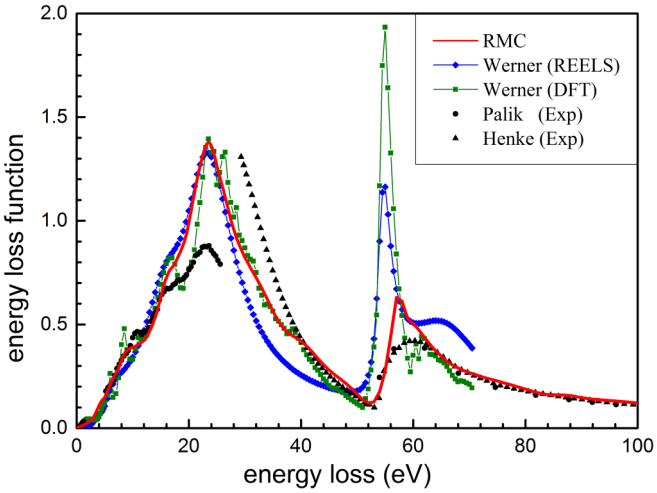

FIG. 4. Comparison of ELFs deduced by the present RMC method with Werner's REELS data and DFT calculation, Palik's compiled data (lacking data in 26–50 eV) and Henke's experiment.

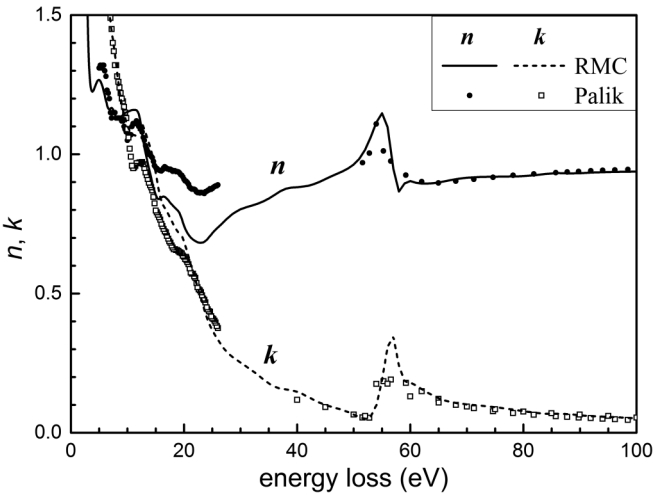

FIG. 5. Comparison on the refractive index n and extinction coefficient k of Fe between the RMC method and Palik's data.

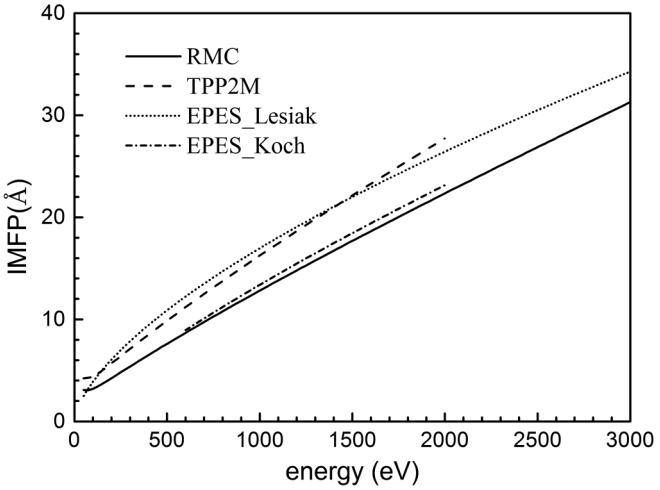

FIG. 6. IMFP as a function of primary electron energy. Solid line: present results by RMC method; dashed line: TPP-2M formula which concides with the data from Refs. [38,43] (not shown here); dotted line: results from EPES measurements by Lesiak; dot-dashed line: results from EPES measured by Koch.

ELF in comparison with the results of Werner *et al.* [12], Palik [1], and Henke *et al.* [37]. In the low energy loss region (<25 eV), the RMC result agrees well with the Werner's data from a deconvolution of REELS spectra while above 15 eV it deviates from Palik's data. In the intermediate energy loss region, i.e., 25–50 eV, our RMC result is closer to Werner's density functional theory (DFT) calculation; meanwhile below 40 eV it deviates from Henke's data which were deduced from atomic scattering factors. In the high energy loss region, the present ELF is very close to Henke's data but has a sharper $M_{2,3}$ edge around 55–60 eV and it is not as strong as that of Werner's data by REELS measurement and DFT calculation. We note that the agreement with Henke's data in the high energy loss region is important because the absorption properties of a solid should approach the atomic properties above the ionization edge. Thus, the present absolute ELF generally falls into the data distribution range from different sources. It agrees with Werner's REELS data in the low energy loss region, with the first-principle DFT calculation in the intermediate energy loss region and with the atomic data in the high energy loss region.

Finally, optical constants are obtained with ELF by using Eq. (9) in Sec. II. Figure 5 displays the calculated refractive index n and extinction coefficient k of Fe in the photon energy range of 0–100 eV, in comparison with Palik's database of optical constants. In addition to the perfect agreement with the experimental data in the high energy loss region, our data also join smoothly the extinction coefficient k of Palik's database in the absent range of 26–40 eV. Furthermore, the IMFP, one of the most important parameters for chemical quantification by surface electron spectroscopy techniques, was calculated with the obtained ELF by adopting a dielectric response theory [38]. The calculated IMFP was then compared with the NIST IMFP database [39] in Fig. 6. A systematic deviation of about 5 Å (relative error 20%−30%) from the Tanuma-Powell-Penn (TPP-2M) formula [40] in the electron energy of 500–2000 eV was found. Though the TPP-2M result is closer to the data obtained from the EPES measurements by Lesiak *et al.* [41], our results agree with another EPES measurement by Koch [42]. We note that such systematic deviation is a direct result of the difference between the present ELF and that of Palik, which was adopted for the fitting procedure of the empirical TPP-2M formula. We note also that by virtue of a comprehensive description of the experiment, REELS excels over EPES in that the IMFP can be determined in the whole energy range in principle with one measurement of the REELS spectrum at one primary energy. Though practically one prefers to perform several REELS measurements at several primary energies for averaging, for EPES separate measurements at the required primary energies are inevitable.

V. SUMMARY

We have obtained ELF and optical constants of iron in the energy range of 0–100 eV from the measured REELS spectra with the help of the recently developed RMC method. The f- and ps-sum rules for the energy averaged ELF are, respectively, 25.99 and 1.04 with relative errors of −0.038% and 4.0%. The ELF used in the REELS spectrum simulation is approximated as the sum of the Drude-Lindhard type functions whose parameters are determined by a global optimization with a MCMC method. The optimization procedure modulates the simulated REELS spectrum to approach the measured one. A combination of a spatially varying DIIMFP derived under the semiclassical framework for electron inelastic scattering along with Mott's cross section for electron elastic scattering was adopted in the Monte Carlo simulation which gives an accurate description of electron transport in a REELS experiment. The advantage of REELS in deriving the IMFP of Fe is demonstrated by comparing the current calculation with NIST IMFP data. The method provides a valid and universal tool to investigate intrinsic optical properties of metals with REELS.

ACKNOWLEDGMENTS

This work was supported by the National Natural Science Foundation of China (Grant No. 11574289) and the Special Program for Applied Research on Super Computation of the NSFC-Guangdong Joint Fund (2nd phase), the Hungarian Scientific Research Fund (OTKA Grants No. NN 103279 and No. K103917), and by the European Cost Actions CM1204 (XLIC) and CM1405 (MOLIM). We also thank the supercomputing center of USTC for support in performing parallel computations.

[1] E. D. Palik, *Handbook of Optical Constants of Solids* (Academic, New York, 1985).
[2] E. D. Palik, *Handbook of Optical Constants of Solids* (Academic, New York, 1991), Vol. II.
[3] L. Feldkamp, L. C. Davis, and M. B. Stearns, Phys. Rev. B **15**, 5535 (1977).
[4] R. F. Egerton, *Electron Energy Loss Spectroscopy in the Electron Microscope*, 2nd ed. (Plenum Press, New York, 1986).
[5] J. Daniels, C. V. Festenberg, H. Raether, and K. Zeppenfeld, *Optical Constants of Solids by Electron Spectroscopy* (Springer, New York, 1970).
[6] F. Yubero, J. M. Sanz, E. Elizalde, and L. Galan, Surf. Sci. **237**, 173 (1990).
[7] J. C. Ingram, K. W. Nebesny, and J. E. Pemberton, Appl. Surf. Sci. **45**, 247 (1990).
[8] F. Yubero, S. Tougaard, E. Elizalde, and J. M. Sanz, Surf. Interface Anal. **20**, 719 (1993).
[9] H. Yoshikawa, Y. Irokawa, and R. Shimizu, J. Vac. Sci. Technol. A **13**, 1984 (1995).
[10] T. Nagatomi, T. Kawano, and R. Shimizu, J. Appl. Phys. **83**, 8016 (1998).
[11] W. S. M. Werner, Appl. Phys. Lett. **89**, 213106 (2006).
[12] W. S. M. Werner, K. Glantschnig, and C. Ambrosch-Draxl, J. Phys. Chem. Ref. Data **38**, 1013 (2009).
[13] H. Jin, H. Shinotsuka, H. Yoshikawa, H. Iwai, S. Tanuma, and S. Tougaard, J. Appl. Phys. **107**, 083709 (2010).
[14] B. Da, S. F. Mao, Y. Sun, and Z. J. Ding, e-J. Surf. Sci. Nanotechnol. **10**, 441 (2012).
[15] B. Da, Y. Sun, S. F. Mao, Z. M. Zhang, H. Jin, H. Yoshikawa, S. Tanuma, and Z. J. Ding, J. Appl. Phys. **113**, 214303 (2013).
[16] D. Tahir, J. Kraaer, and S. Tougaard, J. Appl. Phys. **115**, 243508 (2014).
[17] S. Tougaard and I. Chorkendorff, Phys. Rev. B **35**, 6570 (1987).
[18] W. S. M. Werner, Surf Sci. **526**, L159 (2003).
[19] F. Yubero and S. Tougaard, Phys. Rev. B **46**, 2486 (1992).
[20] Y. C. Li, Y. H. Tu, C. M. Kwei, and C. J. Tung, Surf. Sci. **589**, 67 (2005).
[21] Z. J. Ding and R. Shimizu, Phys. Rev. B **61**, 14128 (2000).
[22] R. Shimizu and Z. J. Ding, Rep. Prog. Phys. **55**, 487 (1992).
[23] R. H. Ritchie, Phys. Rev. **106**, 874 (1957).
[24] G. Gergely, M. Menyhard, G. T. Orosz, B. Lesiak, A. Kosinski, A. Jablonski, R. Nowakowski, J. Tóth, and D. Varga, Appl. Surf. Sci. **252**, 4982 (2006).
[25] W. S. M. Werner, W. Smekal, C. Tomastik, and H. Störi, Surf. Sci. **486**, L461 (2001).
[26] C. M. Kwei, C. Y. Wang, and C. J. Tung, Surf. Interface Anal. **26**, 682 (1998).
[27] Y. F. Chen and C. M. Kwei, Surf. Sci. **364**, 131 (1996).
[28] Z. J. Ding, J. Phys.: Condens. Matter **10**, 1733 (1998).
[29] Z. J. Ding, J. Phys.: Condens. Matter **10**, 1753 (1998).
[30] B. Da, S. F. Mao, and Z. J. Ding, J. Phys.: Condens. Matter **23**, 395003 (2011).
[31] N. F. Mott, Proc. R. Soc. London, Ser. A **124**, 425 (1929).
[32] Z. Czyzewski, D. O. MacCallium, A. Romig, and D. C. Joy, J. Appl. Phys. **68**, 3066 (1990).
[33] R. A. Bonham and T. G. Strand, J. Chem. Phys. **39**, 2200 (1963).
[34] R. H. Ritchie and A. Howie, Philos. Mag. **36**, 463 (1977).
[35] S. Kirkpatrick, C. D. Gelatt, and M. P. Vecchi, Science **220**, 671 (1983).
[36] L. Kövér, D. Varga, I. Cserny, J. Tóth, and K. Tökési, Surf. Interface Anal. **19**, 9 (1992).
[37] B. L. Henke, E. M. Gullikson, and J. C. Davis, At. Data Nucl. Data Tables **54**, 181 (1993).
[38] C. M. Kwei and Y. F. Chen, Surf. Sci. **293**, 202 (1993).
[39] C. J. Powell and A. Jablonski, *NIST Electron Inelastic-Mean-Free-Path Database*, Version 1.2, SRD 71 (National Institute of Standards and Technology, Gaithersburg, MD, 2010).
[40] S. Tanuma, C. J. Powell, and D. R. Penn, Surf. Interface Anal. **17**, 911 (1991).
[41] B. Lesiak, L. Zommer, A. Kosinski, A. Jablonski, G. Gergely, M. Menyhard, A. Sulyok, A. Konkol, Cs. Daroczi, and P. Nagy, in *Proceedings of ECASIA 95* (Wiley, Chichester, 1996), p. 619.
[42] A. Koch, Ph.D. thesis, Eberhard-Karls-Universität, 1996.
[43] W. H. Gries, Surf. Interface Anal. **24**, 38 (1996).